ORIGINAL RESEARCH

Does the DSA reconstruction kernel affect hemodynamic predictions in intracranial aneurysms? An analysis of geometry and blood flow variations

P Berg,[1] S Saalfeld,[2] S Voß,[1] T Redel,[3] B Preim,[2] G Janiga,[1] O Beuing[4]

▸ Additional material is published online only. To view please visit the journal online (http://dx.doi.org/10.1136/neurintsurg-2017-012996).

[1]Department of Fluid Dynamics and Technical Flows, University of Magdeburg, Magdeburg, Germany
[2]Department of Simulation and Graphics, University of Magdeburg, Magdeburg, Germany
[3]Siemens Healthcare GmbH, Forchheim, Germany
[4]Institute of Neuroradiology, University Hospital Magdeburg, Magdeburg, Germany

Correspondence to
Dr P Berg, Department of Fluid Dynamics and Technical Flows, University of Magdeburg, Magdeburg 39106, Germany; berg@ovgu.de

Received 15 January 2017
Revised 29 March 2017
Accepted 13 April 2017

To cite: Berg P, Saalfeld S, Voß S, *et al*. *J NeuroIntervent Surg* Published Online First: [*please include* Day Month Year] doi:10.1136/neurintsurg-2017-012996

ABSTRACT

Background Computational fluid dynamics (CFD) blood flow predictions in intracranial aneurysms promise great potential to reveal patient-specific flow structures. Since the workflow from image acquisition to the final result includes various processing steps, quantifications of the individual introduced potential error sources are required.

Methods Three-dimensional (3D) reconstruction of the acquired imaging data as input to 3D model generation was evaluated. Six different reconstruction modes for 3D digital subtraction angiography (DSA) acquisitions were applied to eight patient-specific aneurysms. Segmentations were extracted to compare the 3D luminal surfaces. Time-dependent CFD simulations were carried out in all 48 configurations to assess the velocity and wall shear stress (WSS) variability due to the choice of reconstruction kernel.

Results All kernels yielded good segmentation agreement in the parent artery; deviations of the luminal surface were present at the aneurysm neck (up to 34.18%) and in distal or perforating arteries. Observations included pseudostenoses as well as noisy surfaces, depending on the selected reconstruction kernel. Consequently, the hemodynamic predictions show a mean SD of 11.09% for the aneurysm neck inflow rate, 5.07% for the centerline-based velocity magnitude, and 17.83%/9.53% for the mean/max aneurysmal WSS, respectively. In particular, vessel sections distal to the aneurysms yielded stronger variations of the CFD values.

Conclusions The choice of reconstruction kernel for DSA data influences the segmentation result, especially for small arteries. Therefore, if precise morphology measurements or blood flow descriptions are desired, a specific reconstruction setting is required. Furthermore, research groups should be encouraged to denominate the kernel types used in future hemodynamic studies.

INTRODUCTION

Computational fluid dynamics (CFD) is a valuable tool to study blood flow and its influence on pathophysiologic processes —for example, in intracranial aneurysms (IA). With increasing hardware performance, studies aimed at understanding the development, growth, and rupture risk of IA have become numerous during the last two decades.[1–4] However, acceptance of the method is still disputed among physicians[5 6] because several assumptions, which often do not reflect patient-specific hemodynamic conditions, are required for CFD and high-quality validation studies are lacking.[7–9] The most important input for personalized CFD simulation is the three-dimensional (3D) model description of the related vessel segment including the aneurysm. To obtain a highly accurate model description that stands at the beginning of the complete workflow, selection of image modality, image acquisition, and image post-processing are very important and may introduce sources of errors. One source of error is the choice of the imaging modality. Geers *et al*[10] studied its influence on CFD results by comparing CT angiography (CTA) and 3D rotational angiography (3D RA). They found equivalent predictions of the qualitative flow characteristics but significant discrepancies in the quantitative measurements. Imaging-dependent neck size differences were reported by Brinjikji *et al*[11] and Schneiders *et al*.[12] They demonstrated—based on two-dimensional (2D) digital subtraction angiography (DSA) and 3D RA comparisons—that significant deviations regarding dome-to-neck ratio, wall shear stresses (WSS), and flow structures may occur.

Also, post-processing of the image datasets required prior to CFD—in particular reconstruction and segmentation—has the potential for uncertainties. O'Meara *et al*[13] compared such kernels for CTA images and found that reconstructions with smooth kernels resulted in an overestimation of the aneurysm neck measurements. These studies illustrate that every single step during the post-processing needs to be addressed to reduce uncertainties and thus to increase the acceptance of CFD in the medical community. However, until now only our initial study provides an analysis of the complete workflow.[14] In this study, qualitative kernel-dependent differences were presented for four patient-specific IAs. To further quantify these initial observations and emphasize the importance of careful image reconstruction, the present work investigates the impact of different 3D RA reconstruction kernels on the variability of the segmentation results and evaluates the hemodynamic predictions using CFD. Eight patient-specific datasets were reconstructed using six different reconstruction settings each. Hence, segmentation and time-dependent hemodynamic results of 48 configurations were quantified to demonstrate the uncertainty that may already occur in the earliest stage of the workflow.

MATERIALS AND METHODS

Case descriptions

Eight saccular IA in seven female patients and one male patient were investigated (see figure 1). Their

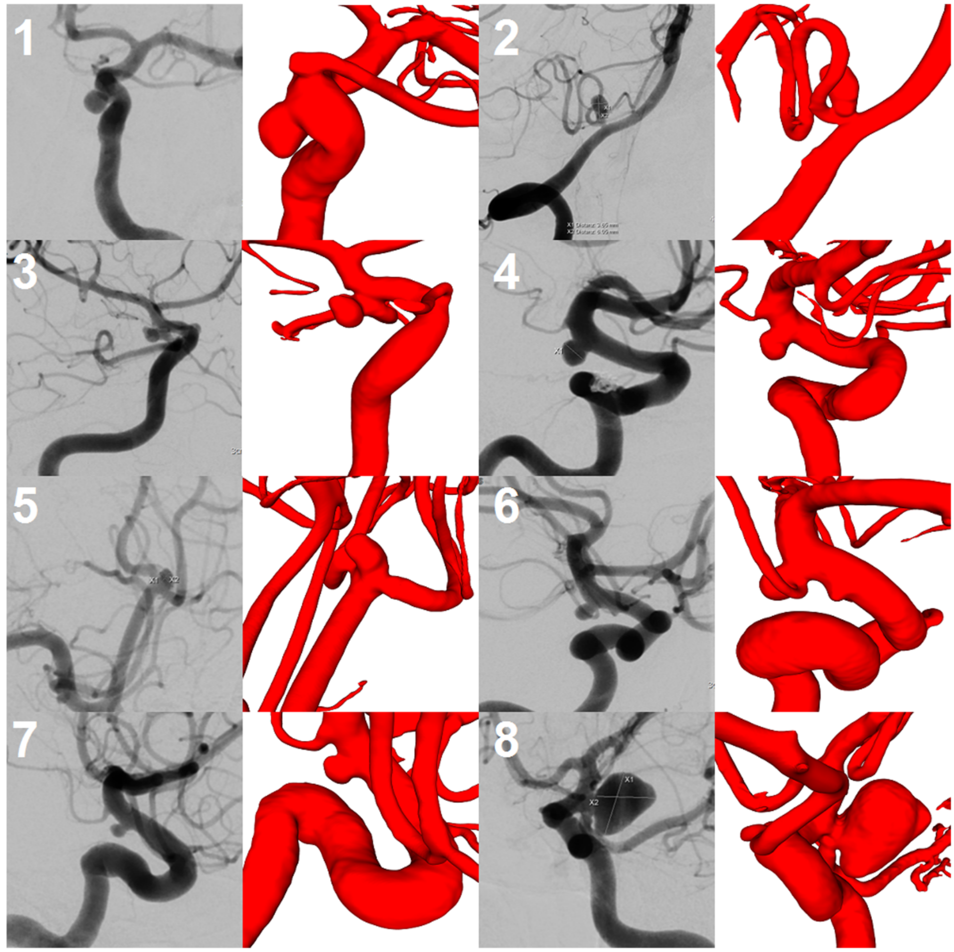

Figure 1 Digital subtraction angiography (DSA) images of the eight aneurysms (left), and the corresponding three-dimensional reconstructions in a magnified view (right). In these cases, an edge-enhanced reconstruction kernel was used.

ages ranged between 45 and 59 years (mean 51 years). Six patients presented with an acute subarachnoid hemorrhage due to aneurysm rupture. In three of these, the clinical condition was poor (Hunt and Hess grade IV), while the other three exhibited no significant neurologic deficits (Hunt and Hess grade I and II, respectively). The locations of the aneurysms were the internal carotid artery (n=1), posterior communicating artery (n=2), anterior choroidal artery (n=2), bifurcation of the middle cerebral artery (n=1), the anterior communicating artery (n=1), and the posterior inferior cerebellar artery (n=1). Their largest diameters varied from 2.8 to 8.0 mm (mean 4.6 mm). Only two aneurysms were larger than 5 mm. All aneurysms were successfully treated with endovascular coiling. The study was performed in accordance with the guidelines of the local ethics authorities.

Imaging and reconstruction

3D imaging was performed on an Artis Q angiography system (Siemens Healthcare GmbH, Forchheim, Germany) and data reconstruction was done on a syngo X Workplace (Siemens Healthcare GmbH) in subtracted manner. After initial reconstruction, all eight datasets underwent secondary reconstructions with different modes. This includes two kernel settings (HU: Hounsfield Units or EE: Edge Enhanced) as well as three different image characteristics (normal, sharp, and smooth). The reconstruction kernel is essential for the resulting 3D images. The EE kernel is the basic recommendation for high contrast applications with injection of iodine. Otherwise, the HU kernel is recommended. The HU kernel is used for quantitative measurements and for DynaCT data. A special algorithm 'smears' out artifacts in the smooth setting. Artifacts are suppressed, but spatial resolution is also reduced. In the sharp setting, spatial resolution is maximized, but results in a higher noise level. The normal setting is a compromise between the sharp and smooth settings and is mostly used for high contrast applications.[15]

For all 3D image reconstructions, isotropic voxel sizes between 0.137 mm and 0.151 mm were chosen. By selecting a voxel size below 0.25 mm, it is ensured that the maximum spatial resolution given by the acquisition setting was not sacrificed by the selection of the voxel size within the reconstruction.

Segmentation

For data segmentation, a threshold-based algorithm is employed. The threshold value is empirically determined by analyzing its corresponding isocontour in the 2D slices of the 3D DSA data as well as the resulting 3D isosurface. The segmentation was checked by an experienced neuroradiologist and compared with the 2D angiographies to ensure plausibility of the extracted shape. First, the segmentation based on the HU normal kernel was separately carried out for each case and used as the reference segmentation. Next, a representative slice of the 3D DSA data comprising the aneurysm was selected and threshold values for the remaining reconstruction kernels were manually adapted such that the resulting isocontours matched the reference segmentation (see online supplementary table S1). Online supplementary figure 1 illustrates the segmentation process (see also Glaßer *et al*[14] for further details).

Thus, a similar aneurysm shape is obtained for each dataset independent of the reconstruction kernel. The chosen threshold value directly influences the segmentation result—that is, lower threshold values comprise more voxels with lower intensity values and yield larger aneurysm and vessel volumes. However, due to the adaptation of all segmentations to the reference segmentation, the major trends between the segmentation differences and thus between the kernel influences can be still obtained, as shown in online supplementary figure 1C and D). The kernel influences the local shape of the aneurysm (see online supplementary figure 1E and F). Thus, adapting the thresholds to the reference segmentation yields similar aneurysm volumes but variations due to local changes. Based on the chosen thresholds, isosurfaces are extracted and converted into triangle surface meshes with MeVisLab 2.7 (MeVis Medical Solutions AG, Bremen, Germany). To avoid variations due to post-processing steps, no smoothing or mesh modification is applied.

Hemodynamic simulations

All segmented aneurysm geometries were imported into a clinical research prototype (Siemens Healthcare GmbH, not for diagnostic use). Afterwards, hemodynamic simulations were carried out using a Lattice–Boltzmann solver. This approach is particularly suitable for the current study since no body-fitted mesh is required. In particular, the noisy surface of datasets reconstructed with sharp kernels would otherwise lead to an inadequate mesh quality. An element size of 0.1–0.15 mm was defined to ensure sufficient mesh resolution.[16] Hence, the minimum ostium diameter of each aneurysm was covered by at least 20 voxels, which leads to mesh-independent velocity results. The total number of voxels ranged from 95 000 to 568 000, the variations being a consequence of the different dimensions of the investigated vessel sections.

To ensure comparability, the same time-dependent velocity profile of a representative idealized flow curve was defined at each of the 48 inlets (see online supplementary figure 2) and traction-free conditions were set at the outlets. Naturally, depending on the individual vessel diameter given by the chosen reconstruction setting at the inlet, the time-dependent inflow rate will vary slightly for each configuration. However, the Reynolds numbers varied only marginally among the different modes of each case (1.2% on average). Furthermore, blood was treated as a laminar incompressible Newtonian fluid.[17] To obtain a periodic solution, two cardiac cycles were simulated for each configuration, while only the last was chosen for analysis.

Analyses

For each case the ostium areas were extracted and compared with respect to size and shape. Furthermore, vessel diameters along the parent artery were computed and the median diameter for each centerline coordinate was measured. To evaluate the effect on the subsequent hemodynamic predictions, velocity, aneurysm neck inflow rate and WSS variability were assessed. In this regard, qualitative comparisons for peak systolic in-plane velocity magnitudes were carried out for each ostium. Additionally, the mean neck inflow rate for 10 equidistant time steps during the cardiac cycle was computed to account for temporal effects. Finally, velocity values and SDs along the centerline of the parent vessels were quantified.

RESULTS

The reconstruction kernels influence the anatomic depiction of aneurysms. For example, small and mid-sized vessels are not segmented after reconstruction with smooth characteristics, whereas they are clearly visible after the use of sharp characteristics (see online supplementary figure 3C,F). Also, vessel diameters and aneurysm volumes are largest after reconstruction with sharp characteristics and smallest in those datasets where smooth characteristics are applied. Pseudostenoses occur, especially in regions close to bifurcations, which leads to wrong representations of small side branches.

In contrast, the mean surface area of all 48 ostium areas was 12.91% larger after reconstruction with smooth kernels than with normal or sharp kernels (see online supplementary figure 3G).

Also, the average size of the ostium areas was 7.88% larger in the 24 HU-based datasets than in the 24 EE-based segmentations. Exclusion of the 'smearing' smooth characteristic decreases this value to 4.13%. However, the kernel-induced variations in ostium sizes are not constant; they vary between the aneurysms. While some areas only differ by 6.15% (case 2), others exhibit a variation of up to 34.18% (case 1) with no clear tendency regarding the absolute ostium size. Again, exclusion of the smooth characteristic leads to differences of 2.98% and 21.32% for cases 2 and 1, respectively.

The anatomic differences caused by the reconstruction settings have an impact on the simulation results. Although the qualitative results (location of inflow jets, areas with slow or stagnating flow) are similar between the different settings (figure 2), the quantitative measurements differ considerably. The average neck inflow rate through the ostia of each subgroup is 5.6% higher in simulations based on reconstructions with HU kernels (HU: 0.434 mL/s vs EE: 0.411 mL/s). This deviation reduces to 3.39% when only normal and sharp characteristics are included. In accordance, mean neck inflow rates are highest in simulations based on smooth characteristics (smooth: 0.452 mL/s; normal: 0.424 mL/s; sharp: 0.391 mL/s), which corresponds to relative differences of 6.2% and 13.5%, respectively (7.8% without smooth).

To identify temporal effects, the mean neck inflow rates of each case were determined at 10 equidistant time steps during the cardiac cycle (see online supplementary table S2). Smallest differences between the kernel-dependent configurations occur close to peak systole (0.56 s). However, the highest differences are not present at low diastole, but rather appear before and after peak systole. Additionally, the relative cycle-averaged SDs of the mean inflow rate vary intra-individually. While the variability in patient 1 was only 5.17%, it was 18.56% in patient 2 (mean of 11.09% for all patients).

Figure 3 illustrates the effect of the reconstruction process on the distribution and size of areas with high/low WSS. The intra-individual differences of the mean time-averaged WSS range from 6.71% to 35.96%, and the maximum time-averaged WSS differs intra-individually between 2.81% and 24.79% (see online supplementary table S3 for detailed information).

The quantification of centerline-based diameters and velocities during peak systole further confirms the observed variability. Only small differences in the median vessel diameter cause considerable deviations with respect to the CFD predictions (figure 4). Despite clear visual differences between the segmentations, in six of eight patients the velocity predictions correlated well, mostly in the proximal part of the parent artery. However, with increasing distance from the inlet cross-sections and decreasing vessel diameters, the differences in the centerline velocity values increased. In particular, stronger mismatches occur distal to each aneurysm. Overall, the centerline-based velocity SD ranged between 3.78% and 6.34% with a mean value of 5.07% for all cases.

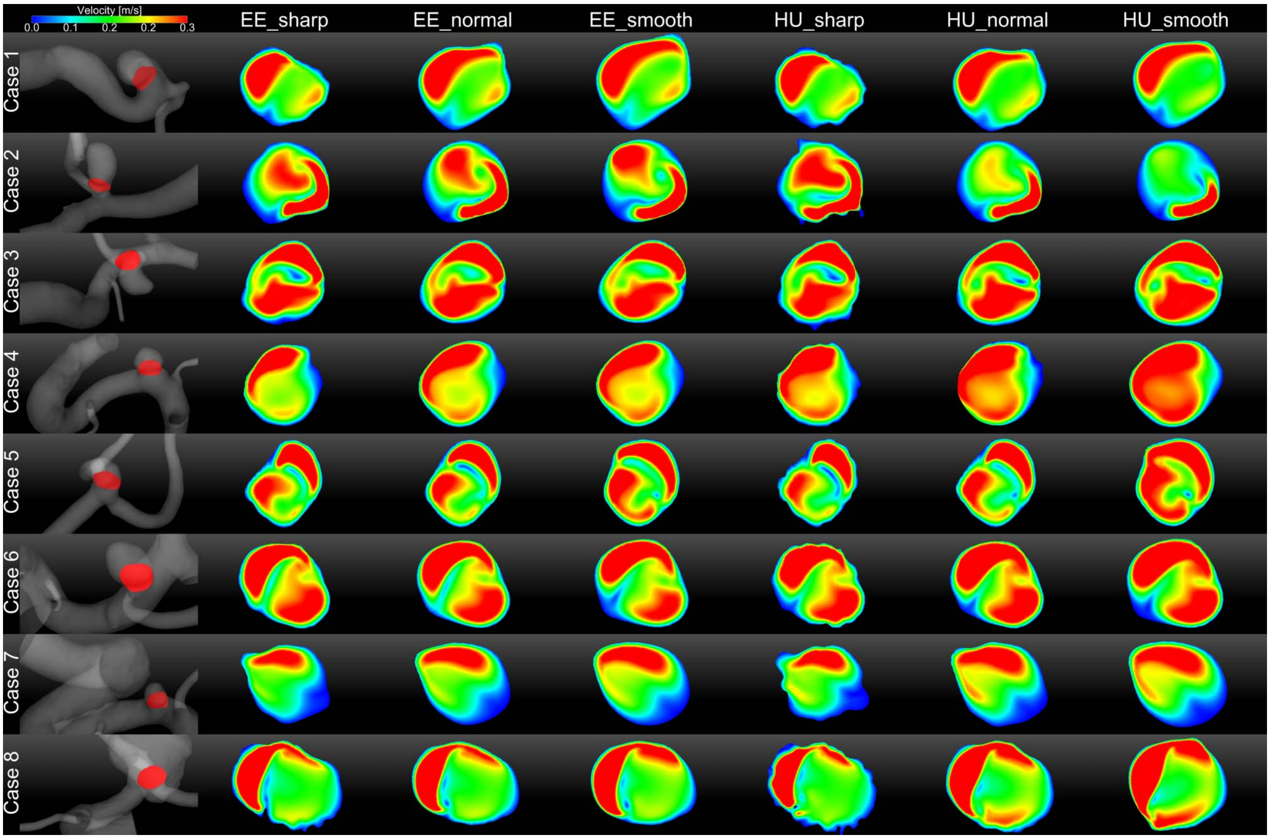

Figure 2 Peak systolic velocity magnitude at the ostia of the eight patient-specific aneurysms (from top to bottom). The illustration allows a qualitative in-plane comparison of hemodynamic predictions using six available reconstruction kernels (from left to right). Notice that, in six of the eight patients (cases 3–8), the absolute velocity magnitude values were higher in those datasets reconstructed with smooth characteristics due to smaller diameters. Furthermore, cases based on Hounsfield Units (HU) reconstructions show generally higher velocities than Edge Enhanced (EE)-based segmentations.

To investigate whether geometric and hemodynamic parameters depend on each other, local SDs for the median diameter and the centerline-based velocity magnitude, respectively, were compared. However, as illustrated in figure 4 (third and sixth row), no clear correlation that applies to all considered cases can be identified.

DISCUSSION

CFD is an established method for the investigation of flow in various fields of technical applications. It also offers the possibility to investigate physiological processes, in particular blood flow. This explains the fact that numerous studies on flow in IA have recently been published. The goal was often to expand the understanding of the development, the growth, and finally the rupture of aneurysms.[18] Additionally, complications or treatment failure after implantation of flow diverters were investigated.[19 20] However, the studies yielded contradictory results, which can at least be partly attributed to methodological differences.[7 8] Overall, in view of the number of publications, little work has been done on how strong the influence of the individual steps of the acquisition and subsequent processing of image datasets on hemodynamic simulations actually is and what consequences must be drawn for further research.

References to the fact that the imaging modality already influences the simulation results are reported by Geers *et al*[10] and Schneiders *et al.*[12] They found that the main flow properties of IA, which were imaged with both CTA and 3D RA, differed very little. On the other hand, they observed great differences in the quantitative measurements. For example, the mean difference in sac-averaged WSS between aneurysms was 44%. Furthermore, aneurysm neck size overestimation due to 3D RA can lead to significantly different WSS results and a different flow structure classification. Other groups reported that the vascular anatomy has the greatest influence on the development of IA and subsequent rupture,[21 22] whereas other factors such as viscosity play only a minor role.[23 24] However, these results are based on a small number of IAs and must therefore be considered with caution. Additionally, they only partially illuminate the aspects of the complex processes involved in hemodynamic simulations. Nevertheless, they were the motivation to further determine and, above all, to quantify the influencing variables. Since O'Meara *et al*[13] showed that the algorithm used for image reconstruction is a significant parameter, it was the focus of this study. Its importance with respect to the intra-aneurysmal flow is confirmed by the results of this study, which was motivated by findings of a preliminary work.[14] These were based on 3D-DSA, reconstructed with two different kernels and three different image characteristics. The segmentation of those datasets reconstructed with smooth characteristics was accompanied by pseudostenoses, which in turn led to significant changes in the flow velocities. Also, the use of these smooth settings led to a minimum vessel size, and the aneurysm volumes were smallest while the ostium area was larger compared with normal or sharp characteristics. As a consequence, the aneurysm neck inflow rates, centerline velocities as well as cycle-averaged WSS

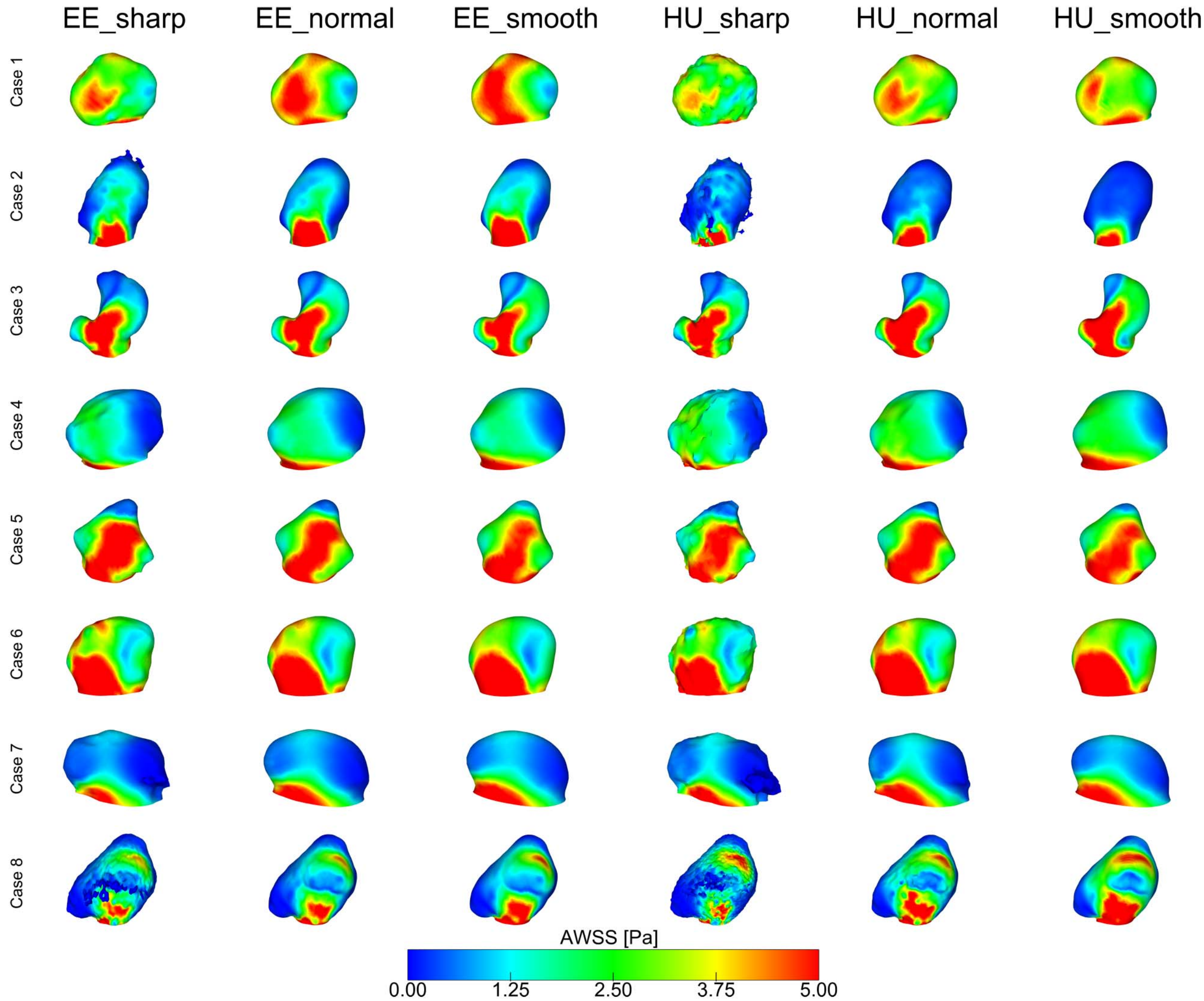

Figure 3 Time-averaged wall shear stresses (AWSS) for each of the 48 investigated aneurysms. Qualitative agreements of the overall stress patterns can be seen, as well as clear deviations with respect to the surface representation.

varied considerably. Based on these findings, smooth settings may be excluded.

It needs to be tested whether the reconstruction setting has an effect on other quantitatively measurable and clinically relevant parameters as well, since this may in turn have a significant impact on treatment planning—for example, for the implantation of a flow diverter. The correct assessment of the probability of rupture of a given aneurysm is also endangered thereby.

To date, no results are available in this study to make a recommendation for best kernel or characteristics. The manufacturer (Siemens Healthcare GmbH) recommends a voxel size down to 0.25 mm using HU kernel and sharp characteristics in high-contrast applications if spatial resolution is to be optimized.[15]

The present work has some limitations. Generally, the segmentation of the aneurysm is adapted to the reference segmentation based on HU normal, so the selection of respective kernels does not influence the segmentation of the aneurysm but only the parent vasculature. Here the influence of the selected kernel using similar threshold levels has to be investigated. Second, in this work a global threshold-based method of segmentation was used, although more advanced approaches exist.[25–27] However, the applied approach corresponds to the general practice and is used by the vast majority of researchers in this field.[28 29] Furthermore, O'Meara *et al*[13] report an overestimation of aneurysm neck, width, and aspect ratio measurements for smooth kernels compared with sharp kernels for 64-row CTA reconstruction. Our study presents similar results with regard to ostium areas. As a consequence, edge enhancing kernels may yield anatomically more accurate reconstructions at the expense of more complex surface models. Since threshold-based segmentations were employed, a comparison of kernel effects versus segmentation technique effects is beyond the scope of this paper. For future work, a systematic analysis could also comprise gradient-based segmentation approaches, which have to be adapted to a reference segmentation to provide further information about whether surface variations are solely caused by kernel effects or the segmentation approach. Finally, only eight aneurysms were examined, which were randomly selected. Generalizable statements can thus not yet be made on the basis of these results.

The results described here, as well as those of other working groups, suggest the use of sharp reconstruction kernels to achieve the closest possible anatomical representation of IAs. Additionally, the results demonstrate the need to accurately examine and quantify all the steps preceding the hemodynamic simulation of IAs. The final goal must be the development of

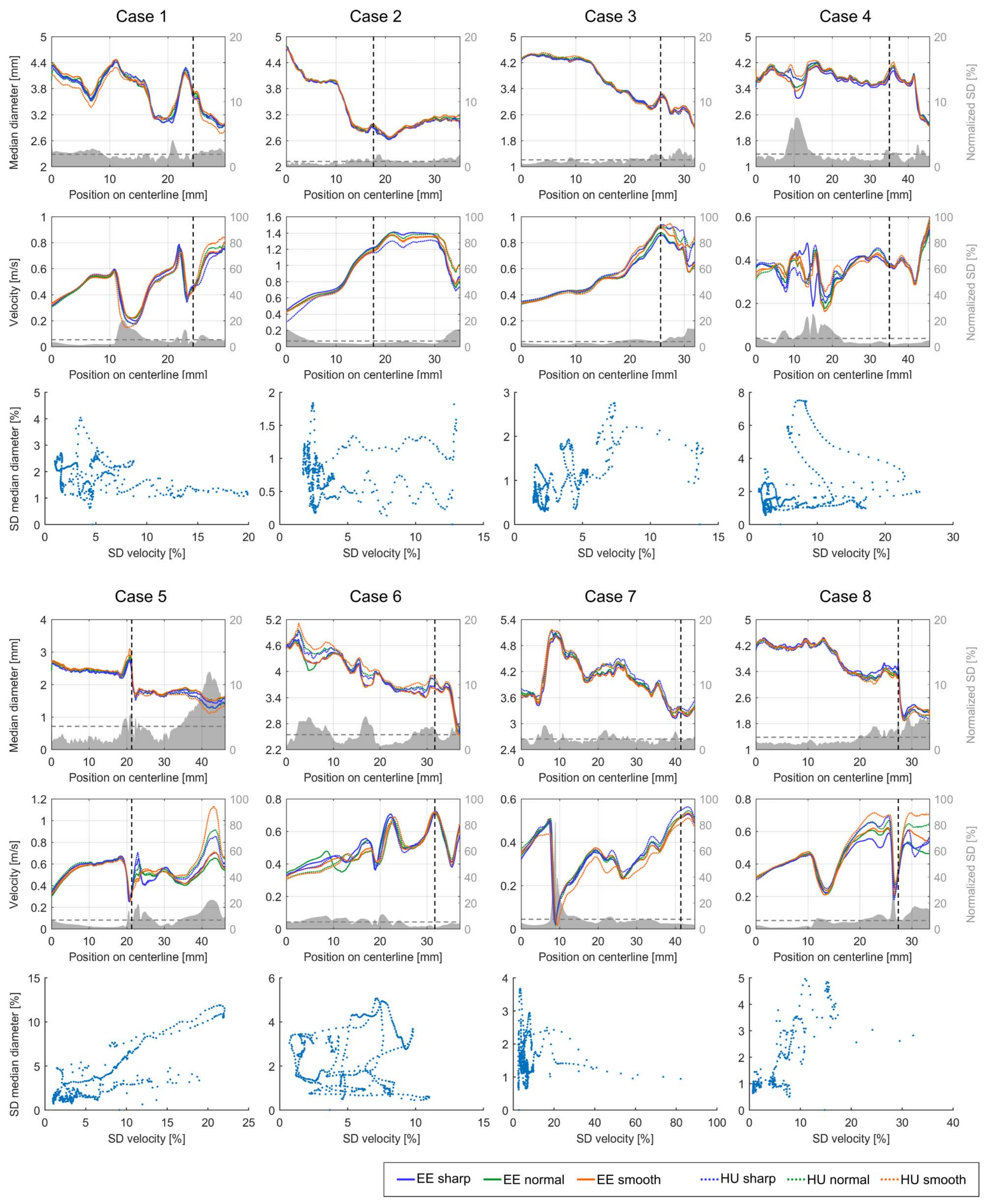

Figure 4 Diameter analysis (first and fourth rows) and peak systolic velocity values (second and fifth rows) along the centerline for each aneurysm. Colors correspond to equivalent characteristic types (ie, sharp, normal, and smooth). Continuous curves represent results for Edge Enhanced (EE)-based reconstructions and dashed curves for Hounsfield Units (HU)-based reconstructions. The normalized SD is plotted in gray for each panel; the dashed horizontal line indicates the mean value. For an improved orientation, a vertical dashed line localizes the centerline position below each aneurysm ostium. To identify the relation between geometric and hemodynamic changes, SDs of the diameter and velocity values at each centerline probe are plotted against each other (third and sixth rows). Note that, with increasing distance from the inlet cross-sections, the differences in the centerline velocity values increase. Only cases 4 and 6 show an opposite trend with deviations in the proximal vessel section. These are caused by artificial indentations of the vessel surface segmentations.

standards that make the work of different research groups comparable and transparent in order to establish the CFD as a diagnostic method and as a therapeutic planning option.

CONCLUSIONS

The choice of reconstruction kernel for 3D DSA data influences the segmentation result, especially for small and perforating arteries as well as aneurysm ostia. This leads to variability in the subsequent numerical flow simulations, which might yield inaccurate conclusions from these results. Hence, if precise morphology measurements or blood flow descriptions are desired, specific care is required to receive realistic values. In order to translate computational methods to a clinical routine, further quantifications of the reconstruction uncertainty are needed. Finally, the authors encourage related research groups to denominate the reconstruction kernel and image characteristics used in their hemodynamic studies to increase the transparency of their modeling techniques.

Acknowledgements The authors acknowledge Dr Steffen Serowy (Department of Neuroradiology, University Hospital Magdeburg, Germany) for his technical assistance regarding the data acquisition.

Contributors Conception and design: PB, SS. Acquisition of data: OB, PB, SS, SV. Analysis and interpretation of data: PB, SS, SV, OB, TR. Drafting the article: PB. Critically revising the article: SS, PB, TR, GJ, BP. Statistical analysis: PB, SS, SV. Administrative/technical/material support: TR, GJ, BP. Study supervision: OB, GJ, BP. Guarantor: PB.

Funding This work was supported by the Federal Ministry of Education and Research in Germany under grant number 13GW0095A.

Disclaimer The concepts and information presented in this paper are based on research and are not commercially available.

Competing interests TR is employee of Siemens Healthcare GmbH.

Patient consent Obtained.

Ethics approval Ethics approval was obtained from University Hospital Magdeburg.

Provenance and peer review Not commissioned; externally peer reviewed.

Data sharing statement Datasets and case-specific geometry and blood flow information are available upon request from the corresponding author.

REFERENCES

1 Chung B, Cebral JR. CFD for evaluation and treatment planning of aneurysms: review of proposed clinical uses and their challenges. *Ann Biomed Eng* 2015;43:122–38.
2 Xiang J, Tutino VM, Snyder KV, *et al*. CFD: computational fluid dynamics or confounding factor dissemination? The role of hemodynamics in intracranial aneurysm rupture risk assessment. *AJNR Am J Neuroradiol* 2014;35:1849–57.
3 Meng H, Tutino VM, Xiang J, *et al*. High WSS or low WSS? Complex interactions of hemodynamics with intracranial aneurysm initiation, growth, and rupture: toward a unifying hypothesis. *AJNR Am J Neuroradiol* 2014;35:1254–62.
4 Janiga G, Berg P, Sugiyama S, *et al*. The Computational Fluid Dynamics Rupture Challenge 2013—Phase I: Prediction of rupture status in intracranial aneurysms. *AJNR Am J Neuroradiol* 2015;36:530–6.
5 Fiorella D, Sadasivan C, Woo HH, *et al*. Regarding "Aneurysm rupture following treatment with flow-diverting stents: computational hemodynamics analysis of treatment". *AJNR Am J Neuroradiol* 2011;32:E95–7; author reply E98–100.
6 Kallmes DF. Point: CFD—computational fluid dynamics or confounding factor dissemination. *AJNR Am J Neuroradiol* 2012;33:395–6.
7 Steinman DA, Hoi Y, Fahy P, *et al*. Variability of computational fluid dynamics solutions for pressure and flow in a giant aneurysm: the ASME 2012 Summer Bioengineering Conference CFD Challenge. *J Biomech Eng* 2013;135:21016.
8 Berg P, Roloff C, Beuing O, *et al*. The Computational Fluid Dynamics Rupture Challenge 2013—Phase II: Variability of hemodynamic simulations in two intracranial aneurysms. *J Biomech Eng* 2015;137:121008.
9 Berg P, Stucht D, Janiga G, *et al*. Cerebral blood flow in a healthy circle of Willis and two intracranial aneurysms: computational fluid dynamics versus four-dimensional phase-contrast magnetic resonance imaging. *J Biomech Eng* 2014;136 (9 pages) Paper No: BIO-13-1247.
10 Geers AJ, Larrabide I, Radaelli AG, *et al*. Reproducibility of image-based computational hemodynamics in intracranial aneurysms: comparison of CTA and 3DRA. *Proceedings of IEEE Symposium on Biomedical Imaging: From Nano to Macro (ISBI)* 2009:610–13.
11 Brinjikji W, Cloft H, Lanzino G, *et al*. Comparison of 2D digital subtraction angiography and 3D rotational angiography in the evaluation of dome-to-neck ratio. *AJNR Am J Neuroradiol* 2009;30:831–4.
12 Schneiders JJ, Marquering HA, Antiga L, *et al*. Intracranial aneurysm neck size overestimation with 3D rotational angiography: the impact on intra-aneurysmal hemodynamics simulated with computational fluid dynamics. *AJNR Am J Neuroradiol* 2013;34:121–8.
13 O'Meara B, Rahal JP, Lauric A, *et al*. Benefit of a sharp computed tomography angiography reconstruction kernel for improved characterization of intracranial aneurysms. *Neurosurgery* 2014;10(Suppl 1):97–105.
14 Glaßer S, Berg P, Voß S, *et al*. From imaging to hemodynamics—how reconstruction kernels influence the blood flow predictions in intracranial aneurysms. *Curr Dir Biomed Eng* 2016;2:679–83.
15 syngo Application Software. *Operator Manual, VD11*. Siemens Healthcare GmbH, 2016.
16 Berg P, Voß S, Becker M, *et al*. Bringing hemodynamic simulations closer to the clinics: a CFD prototype study for intracranial aneurysms. *Proceedings of International Conference of the IEEE Engineering in Medicine and Biology Society (EMBC16)*. 2016:3302–5.
17 Janiga G, Berg P, Beuing O, *et al*. Recommendations for accurate numerical blood flow simulations of stented intracranial aneurysms. *Biomed Tech (Berl)* 2013;58:303–14.
18 Cebral J, Ollikainen E, Chung BJ, *et al*. Flow conditions in the intracranial aneurysm lumen are associated with inflammation and degenerative changes of the aneurysm wall. *AJNR Am J Neuroradiol* 2017;38:119–26.
19 Schneiders JJ, VanBavel E, Majoie CB, *et al*. A flow-diverting stent is not a pressure-diverting stent. *AJNR Am J Neuroradiol* 2013;34:E1–4.
20 Turowski B, Macht S, Kulcsar Z, *et al*. Early fatal hemorrhage after endovascular cerebral aneurysm treatment with a flow diverter (SILK-Stent): do we need to rethink our concepts? *Neuroradiology* 2011;53:37–41.
21 Can A, Mouminah A, Ho AL, *et al*. Effect of vascular anatomy on the formation of basilar tip aneurysms. *Neurosurgery* 2015;76:62–6.
22 Tateshima S, Chien A, Sayre J, *et al*. The effect of aneurysm geometry on the intra-aneurysmal flow condition. *Neuroradiology* 2010;52:1135–41.
23 Morales HG, Larrabide I, Geers AJ, *et al*. Newtonian and non-Newtonian blood flow in coiled cerebral aneurysms. *J Biomech* 2013;46:2158–64.
24 Castro MA, Ahumada Olivares MC, Putman CM, *et al*. Unsteady wall shear stress analysis from image-based computational fluid dynamic aneurysm models under Newtonian and Casson rheological models. *Med Biol Eng Comput* 2014;52:827–39.
25 Firouzian A, Manniesing R, Flach ZH, *et al*. Intracranial aneurysm segmentation in 3D CT angiography: method and quantitative validation with and without prior noise filtering. *Eur J Radiol* 2011;79:299–304.
26 Sen Y, Qian Y, Avolio A, *et al*. Image segmentation methods for intracranial aneurysm haemodynamic research. *J Biomech* 2014;47:1014–19.
27 Boegel M, Hoelter P, Redel T, *et al*. A fully-automatic locally adaptive thresholding algorithm for blood vessel segmentation in 3D digital subtraction angiography. *Conf Proc IEEE Eng Med Biol Soc* 2015;2015:2006–9.
28 Jeong W, Rhee K. Hemodynamics of cerebral aneurysms: computational analyses of aneurysm progress and treatment. *Comput Math Methods Med* 2012;2012:782801.
29 Castro MA. Understanding the role of hemodynamics in the initiation, progression, rupture, and treatment outcome of cerebral aneurysm from medical image-based computational studies. *ISRN Radiol* 2013;2013:602707.

Does the DSA reconstruction kernel affect hemodynamic predictions in intracranial aneurysms? An analysis of geometry and blood flow variations

P Berg, S Saalfeld, S Voß, T Redel, B Preim, G Janiga and O Beuing

J NeuroIntervent Surg published online May 2, 2017